MULTISTATIC RADAR SYNCHRONISATION USING COTS GPS DISCIPLINED OSCILLATORS

Piers J. Beasley[1], Matthew A. Ritchie[2]

Department of Electronic and Electrical Engineering, University College London, UK
E-mail: {piers.beasley.19[1] m.ritchie[2]}@ucl.ac.uk

Keywords: MULTISTATIC RADAR, NETWORKED RADAR, GPSDO, RADAR SYNCHRONISATION

Abstract

The benefits of multistatic radar have been well understood for decades, though the challenges of implementing such systems have limited their development and subsequent operational use. Multistatic radar's performance enhancements, over standard monostatic radar, result from the cooperation and data-fusion between spatially separated radar nodes, however, to enable cooperation and data-fusion, some degree of node-to-node time and frequency synchronisation is critical. In this work, the use of commercial off-the-shelf (COTS) GPS Disciplined Oscillators (GPSDO) as a source of indirect radar synchronisation is evaluated and the development, and subsequent testing, of a GPSDO based radar synchronisation system is presented.

1 Introduction

The use of global satellite navigation signals from constellations such as the GPS has now become a common method for achieving synchronisation across spatially separated systems. GPS Disciplined Oscillators are devices comprising of both a highly stable Local Oscillator (LO), a GPS timing receiver and circuitry for disciplining the LO to the GPS receiver timing output. The works by Sandenbergh et al. provide key references of experimental results within the recent literature on GPSDO based networked radar synchronisation [1, 2, 3]. In these papers, three identical quartz-based GPSDOs were designed to provide an alternative to physical synchronisation cables for the NetRAD [1] and NeXtRAD [4] multistatic radar systems. Comparatively, the paper instead investigates the use of two different COTS GPSDOs that use differing LO technologies, namely, double oven-controlled crystal oscillators (OCXO) versus Rubidium oscillators. For the rest of Section 1, the requirements of coherent multistatic radar synchronisation are introduced. In Section 2, the performance of two different COTS GPSDOs is evaluated, followed by the development of a GPSDO based radar synchronisation system, in Section 3. A preliminary zero-baseline multistatic lab experiment is presented in Section 4, before the conclusions of this work are made in the final section.

1.1 Coherent Radar Synchronisation

The time and frequency synchronisation requirements for coherent bistatic/multistatic radar are well documented in [5, 6, 7]. To summarise, the synchronisation requirements should be derived from the required radar systems performance, additionally, these requirements vary depending on the radar signal processing intended to be operated on the radar data.

1.1.1 Time Synchronisation: A common appreciation of time between transmitter and receiver nodes is fundamental for accurate bistatic range measurements. Any timing error will manifest as a bistatic range error, ΔR_b. The range error can be calculated by $\Delta R_B = \Delta t_B C$, where Δt_B is the time offset between nodes and C is the speed of light. In [7], Willis states a timing accuracy of 1/10 th of the compressed radar pulse width is required. To put said requirement into perspective, a 0.33 ns timing accuracy would be required for a radar system with a 1 m range resolution.

1.1.2 Frequency Synchronisation: Synchronisation of LOs across radar nodes permits the synchronisation of carrier frequencies, base-band sampling and data clocks. Deviation in carrier frequencies across radar nodes will result in Doppler shift errors. A constant deviation in carrier frequency, Δf_c, over the coherent processing interval (CPI) will result in a Doppler error of Δf_c. However, fluctuations of Δf_c during the CPI will result in target Doppler spreading [8]. The maximum acceptable offset in LO frequency is related to the required radial velocity accuracy of the radar system, again, application dependant. However, in general, a frequency offset of less than the velocity resolution, V_r, of the signal processing is acceptable $\Delta f_c < V_r/C$ [6].

1.1.3 Phase Synchronisation: The relative phase stability requirement for LOs is dependent on the duration and type of coherent radar processing required [7]. In a standard monostatic radar, the same LO is used for both up- and down-conversion, permitting significant cancellation of random phase fluctuations and phase noise [9]. Conversely, in bistatic/multistatic radar, separate LOs are used, as such no cancellation of phase noise or spurious signals is experienced; this dramatically increases the performance requirement of the LOs, should a performance equitable monostatic radar be required [1]. Close-in phase noise reduces the Sub Clutter Visibility (SCV) performance of the radar by broadening the noise

floor of the static clutter spectrum, reducing the radar's ability to detect small moving targets in the presence of strong stationary clutter or a large target [9, 6].

1.1.4 Coherent Integration: Coherent pulse integration is often used to increase the SNR of targets in the presence of noise. However, if a carrier frequency offset exists due to a LO frequency offset, a loss of coherent integration gain will be observed, resulting in an SNR loss proportional to the magnitude of the frequency offset [1]. Additionally, the uncorrelated phase noise between the individual matched LOs in the transmitter and receiver also causes a reduction of coherent integration gain.

2 COTS GPSDOs Performance Evaluation

In this section, the relative synchronisation performance of two different models of COTS GPSDO is investigated. One model is the Trimble Thunderbolt E, designed around a double OCXO [10]. The second model is a Spectratime LNRCLOK-1500, which in addition to an OCXO, contains a compact Rubidium frequency reference [11]. Two of each GPSDO are used in this work to allow direct comparison between relative GPSDO-to-GPSDO synchronisation performances across the different LO technologies. As standard for GPSDOs, both devices output a low-jitter 1PPS (Pulse Per Second) signal synchronised to UTC, and a 10 MHz frequency reference that should be, at minimum, syntonised to UTC.

2.1 COTS GPSDOs

Both devices host inbuilt single-carrier GPS receivers that utilise the L1 carrier C/A code available to the Standard Precision Service. The Trimble device hosts a 12-channel Trimble GPS receiver, whereas the Spectratime device hosts a 50-channel U-Blox LEA-6T GPS timing receiver. Theoretically, the maximum number of GPS satellites observable at any single point in time is less than 12, so the main advantage of greater than 12 channels is the reduction of time to first fix. The GPS receivers were set up in an All-in-View configuration, meaning all available satellites are used to determine a time-fix. Comparison between All-in-View and Common-View receiver synchronisation is examined in [12]. In these experiments, the Trimble GPS receivers self-surveyed their position by taking an average of 2000 position fixes. However, the Spectratime devices were found to periodically update the receiver GPS position, indicating they had not self-survey their position to minimise positioning error through averaging.

2.1.1 1PPS to 10 MHz Relationship: The performance and functionality of commercially available GPSDOs can vary considerably between manufacturers, as found by NIST in [13]. Therefore, a series of lab experiments have been conducted to calibrate the performance of the devices used in this work. Both models of GPSDOs 10 MHz reference was found to be syntonised to the 1PPS timing output. The 10 MHz positive zero-crossing of the Trimble devices exhibited a fixed 8.9 ns offset to the 1PPS, which was consistent across the two Trimble devices and sustained power-cycling. Therefore, when the two Trimble GPSDOs 1PPS signals are synchronised, so will the phase of the 10 MHz signals. In contrast, the phase relationship between the Spectratime device's 1PPS and 10 MHz is substantially more complicated. The 1PPS-10 MHz phase was found to be a product of both the power on 1PPS-10 MHz phase, and the error between the free-running 1PPS signal (pre-oscillator disciplining) and the UTC 1PPS (output by the on-board GPS receiver). As a result, more often than not, the 1PPS-10 MHz offset is not common across identical devices. This results in a phase offset of the 10 MHz signals between devices, even when the 1PPS signals are perfectly synchronised. To achieve a common 1PPS-to-10 MHz offset across multiple devices, calibration is first required by comparing the 1PPS and 10 MHz output of each device on an oscilloscope. Assuming the two devices powered on with a common 1PPS-to-10 MHz phase, the 1PPS can be shifted, relative to the 10 MHz, to remove the error introduced when the 1PPS signal is shifted to match the UTC second.

2.2 GPSDO Lab Measurements and Results

The relative frequency synchronisation of the four co-located GPSDOs 10 MHz outputs was measured during a series of lab experiments using a 5 port K+K FXE phase and frequency measurement device. This measurement device has a 1 ps resolution for the 1 s averaging time used in these measurements [14]. Whereas, the relative time synchronisation between the GPSDOs was analysed by comparing the GPSDOs individual 1PPS outputs using a 4-channel RTO2024 oscilloscope, with a time resolution of 100 ps. All four devices were set up in the lab and shared a single GPS antenna feed, split 4-ways using a S14GT-A GPS signal splitter. Identical cable lengths were used where necessary. In the following results, the relative synchronisation between 3 pairings of GPSDOs is presented, namely LNRCLOK 1 vs LNRCLOK 2 (Rb1Rb2), Thunderbolt E 3 vs Thunderbolt E 4 (Q3Q4), and LNRCLOK 1 vs Thunderbolt E 3 (Rb1Q3).

2.2.1 Relative Timing Error: It is expected that there will be a relative, but static time offset between each GPSDO; this offset is a sum of the GPS receiver self-survey error, fixed GPS receiver PPS offset to UTC, and internal GPSDO delays [13, 3]. Figure 1 compares the phase between the pairings of GPSDOs over a 6-day period. Prior to this measurement, the devices were left tracking GPS for a minimum of 2-days in their default manufacture settings. As detailed in Table 1, the largest mean time offset of 16.51 ns was measured between the two Trimble GPSDOs, equivalent to a bistatic range offset of 4.9 m. A mean time offset of 9.4 ns was measured between the two Spectratime devices and 11.1 ns offset was measured between a pairing of an Spectratime and a Trimble, equivalent to range offsets of 2.8 m and 3.4 m respectively. In this 6-day measurement, the relative timing performance of Trimble GPSDOs exceeds that of the Spectratime GPSDOs, indicated by a factor of four smaller standard deviation of 1.46 ns. Additionally, the

maximum time error, relative to the mean time offset, was just 9.88 ns ($\Delta R_B = 3.0m$), compared to the Spectratime devices, which was recorded as 19.60 ns ($\Delta R_B = 5.87m$).

Table 1: Relative timing error statistics for three GPSDO pairings, measured by comparing the co-located GPSDO 1PPS outputs over a 6-day period.

Time offset	Rb1Rb2	Q3Q4	Rb1Q3
Mean (ns)	9.40	16.51	11.1
1σ (ns)	5.72	2.12	6.19
2σ (ns)	11.44	4.24	12.28
Peak (ns)	19.60	9.88	30.04

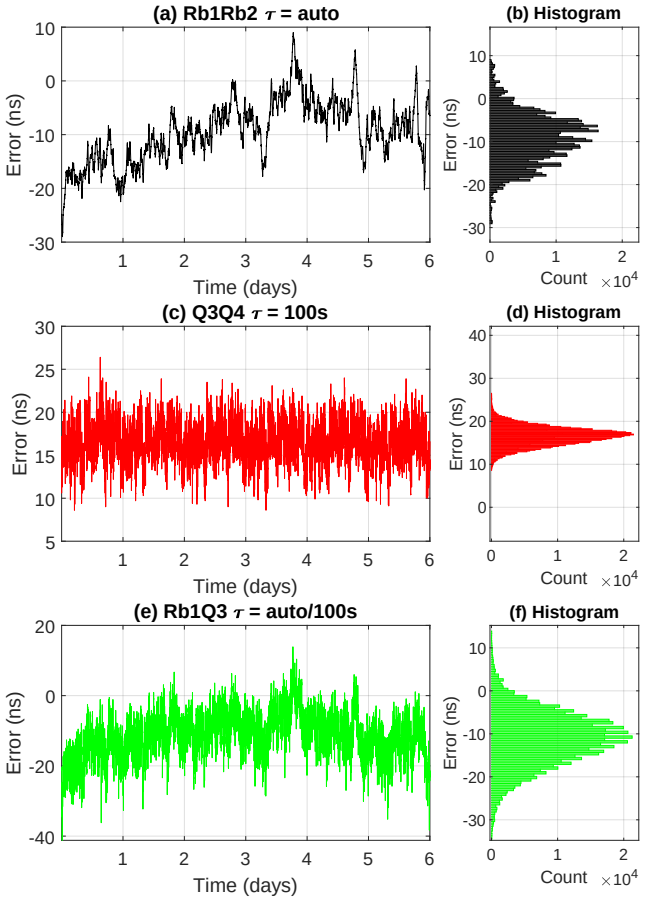

Fig. 1 Plot of relative 1PPS timing errors between co-located GPSDOs for a 6-day period (a) LNRCLOCK, (c) Thunderbolt E, (d) LNRCLOCK vs Thunderbolt E.

2.2.2 Relative Frequency Stability: When tracking GPS, the GPSDO's internal disciplining circuity steers the internal oscillator toward the long-term average of the GPS receiver's PPS timing output. To maximise the frequency stability of the GPSDOs, the disciplining loop time constant should be optimally tuned. This is done by comparing the stability of both the GPS receiver 1PPS output with the stability of the internal oscillator. The time constant defines the point at which the GPSDO adopts the stability of the GPS PPS timing reference, before which the stability is dependent on the internal oscillator [2]. The Trimble devices have a static user-defined disciplining loop time constant and damping factor for adjusting the disciplining loop characteristics, set to 100s and 1 respectively as manufacturer defaults. Whereas, the Spectratime devices employ an adaptive disciplining mechanism that automatically adjusts the time constant by analysing the stability of the GPS PPS timing reference against its highly stable internal Rubidium reference [11]. In Fig. 2, the relative frequency stability of the GPSDO pairs are provided as a function of averaging time. This includes plots of the overlapping Allan Deviation for Rb1Rb2 and Q3Q4 GPSDO pairs during the 284-hour experiment. In these experiments, the disciplining loop characteristics were set to their manufacture defaults. One can observe, the poorer short-to-medium-term stability, for $\sigma_y(\tau < 10^3)$ of the Trimble devices, when compared to the Spectratime devices. This comparative instability is also observable in Fig.1 where there are visibly more high-frequency components in the phase plots of Q1Q2 in Fig.1(c), than in phase plot of Rb1Rb2 in Fig.1(a). To improve the short-to-medium stability of the Trimble devices, the parameters of the Trimble disciplining loops were then optimised. This was achieved by comparing the stability of the internal double-OCXO to an estimated stability of the GPS receivers 1PPS (only an estimate of the GPS receiver's stability could be used, as there is no way to directly sample its output). An estimated optimal time constant of $\tau = 1000s$ was chosen, and a damping factor of 0.707. The relative frequency stability improvement of the Trimble devices, with the adjusted disciplining loop characteristics, can be observed in Fig. 2; an approximate magnitude improvement in short-medium term relative frequency stability was attained. That said, by increasing the time constant, a slight reduction of time accuracy was experienced and the time to reach optimal lock to GPS time was considerably increased to approximately 3.5 hrs.

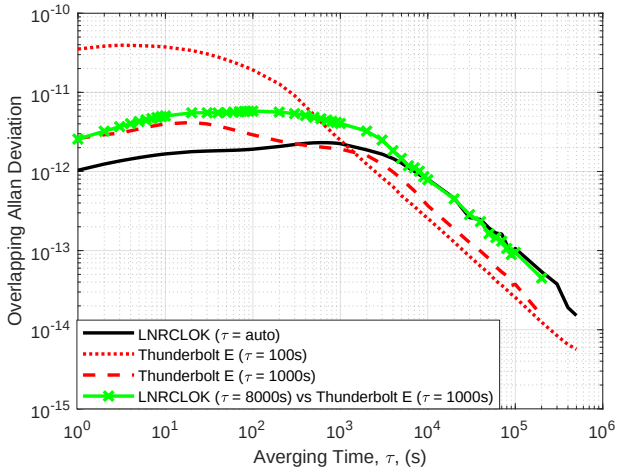

Fig. 2 Plot of Overlapping Allan Deviation comparing the relative frequency stability of co-located GPSDOs 10 MHz outputs versus averaging time, τ.

Table 2: Short-term Overlapping Allan Deviation comparing the relative frequency stability between GPSDO pairings.

τ	Rb1Rb2 $\tau_{PLL} = auto$	Q3Q4 $\tau_{PLL} = 100s$	Q3Q4 $\tau_{PLL} = 1ks$
1	1.03e-12	3.53e-11	2.62e-12
10	1.67e-12	3.75e-11	3.99e-12
100	1.91e-12	1.92e-11	2.91e-12

2.2.3 Relative Frequency Error: Fig.3 illustrates the fractional frequency error between GPSDOs, for a 1s averaging time, over a 119-hour period. This figure permits a better insight into the short-term relative frequency stability of each GPSDO pairing, over a time duration similar to a realistic CPI duration of a radar system. By adjusting the disciplining loop characteristics of the Trimble devices, a frequency syntonisation performance on the same order of magnitude as the Spectratime devices was attained. Using the statistics from Table 3, it can be approximated that, in these ideal co-located lab conditions, for 95.4% of the time a carrier offset of $< 2.42 \times 10^{-11}$ would be achieved for all three GPSDO pairings. This translates to a target velocity error of < 0.007 m/s.

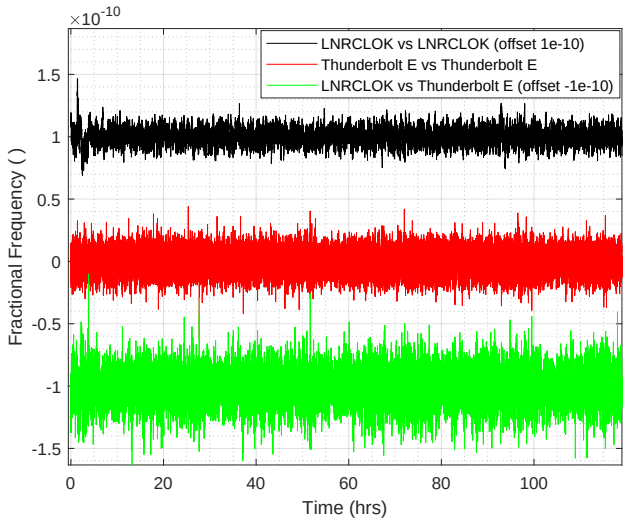

Fig. 3 Relative Fractional frequency offsets, for $\tau = 1s$, between GPSDO pairs for a 119 period. Trimble GPSDOs set up with adjusted disciplining loops.

Table 3: Fractional frequency statistics for $\tau = 1s$, analogous to a coherent integration period in radar signal processing.

FF $\tau = 1s$	Rb1Rb2 $\tau_{PLL} = 8ks$	Q3Q4 $\tau_{PLL} = 100s$	Rb1Q3 $\tau_{PLL} = 8k/1ks$
Mean	3.55e-15	6.13e-14	5.39e-14
1σ	4.56e-12	7.15e-12	1.21e-11
2σ	9.12e-12	1.43e-11	2.42e-11
Max	4.08e-11	5.65e-11	8.99e-11

2.2.4 Relative Phase Noise: A Micro-Semi 5120a phase noise test set was used to measure the relative phase noise performance of the Trimble and Spectratime GPSDOs. Table 4 compares the measured relative performance of the two models. As identical oscillators are used, on the assumption they have the same phase noise, the phase noise of an individual oscillator can be estimated as 3 dB less than the relative value; due to the phase noise being uncorrelated and thus additive.

Table 4: Measured relative phase noise between GPSDOs.

Offset from carrier (Hz)	Rb1Rb2 (dBc/Hz)	Q3Q4 (dBc/Hz)
1	-102	-94
10	-132	-124
100	-144	-136
1,000	-160	-141
10,000	-160	-143
100,000	-160	-143

3 GPSDO Sync System Architecture

3.1 System Architecture

A radar synchronisation system has been developed to clock and trigger three radar systems, namely, the bladeRAD hybrid radar system [15], the ARESTOR multi-role RF system [16], and the NeXtRAD radar system [4]. The GPSDOs alone, described in the previous section, cannot be used to clock and trigger the radars; instead, a system is needed to derive a common trigger signal, provide network control of GPSDOs, and translate the GPSDO frequency reference to meet the input requirements of each radar system. A system comprising of three main pieces of hardware has been designed to meet these requirements. Each system node comprises of a GPSDO, a custom interface card and a Raspberry Pi (RPI). Identical hardware setups will be required at each node, though, the nodes will operate in a master-slave architecture. Figure 4 is a photograph of a single sync system node.

3.1.1 Radar Trigger Derivation: The synchronous 1PPS output of the GPSDOs can be used to derive a low jitter trigger signal for synchronisation of acquisitions across multiple radar nodes. This can be achieved by allowing a common single 1PPS pulse to pass at all nodes, see figure 5. This solution results in the trigger accuracy that is only constrained by the degree of error between the GPSDOs 1PPS outputs, plus the skew introduced by the analogue trigger circuitry. The skew introduced by the analogue trigger circuitry has been measured to be less than 0.15 ns, with a standard deviation of 12.1 ps, negligible in comparison to the measured 1PPS synchronisation errors between GPSDOs.

3.1.2 Frequency Reference Conversion: The 10 MHz clock signal requires conversion to meet the external clock input

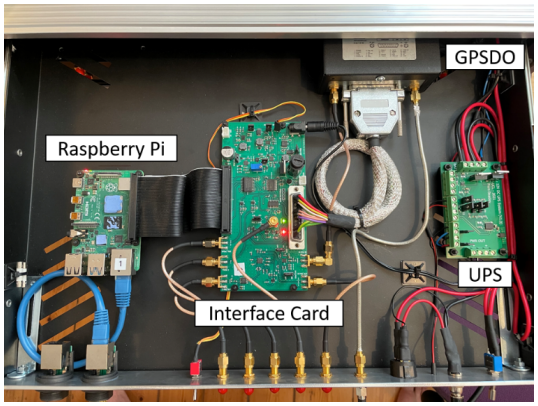

Fig. 4 Photograph of a single node of the GPSDO based radar synchronisation system, ruggedised into a single 1U 19" rack shelf.

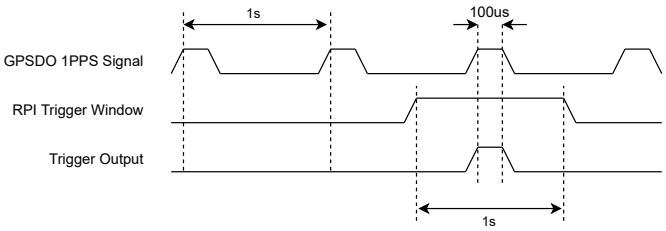

Fig. 5. GPSDO Sync System Trigger Timing Diagram

requirements of the radar systems; said conversion is implemented on the custom interface cards. In the case of the bladeRAD and NeXtRAD systems, a 10 MHz 3.3V CMOS signal is derived from the GPSDOs 10 MHz sinusoidal signal using a simple clock buffer. However, the ARESTOR system requires a 5 MHz 3.3V CMOS signal, a slightly more complex task due to the need to synchronise the edge of the 10 MHz input signal, used for generation of the 5 MHz, across multiple interface cards. This is necessary to avoid a 10 MHz period of clock error between ARESTOR nodes.

4 ARESTOR Radar Measurement

The radar synchronisation system was tested during a series of zero-baseline short-range lab experiments with the ARESTOR multi-functional radar system. The ARESTOR system was set up in a pseudo-multistatic configuration, where a single ARESTOR node acted as a monostatic transceiver and a second ARESTOR node acted as a purely passive receiver. The radar was configured in an FMCW mode with a PRF of 1 kHz, chirp duration of 0.1 ms, and transmitted a 160 MHz linear-frequency-modulated up-chirp centred on 2.42 GHz. Individual GPSDO sync system nodes were configured for each radar node. In these initial experiments, the Spectratime GPSDOs were used as a reference to derive the clock and trigger signals for each radar node. In these results, the direct breakthrough was used for analysis of the node-to-node synchronisation. Fig.6 is the bistatic range-time-intensity (RTI) plot for a 15-minute experiment conducted to measure the relative synchronisation between the nodes when disciplined to co-located GPSDOs. One can observe that at the start of the capture the direct path breakthrough is offset by a single range bin (0.83 m), indicating a time offset of approximately 2.8 ns between radar trigger times. As the capture progresses the breakthrough migrates a further 2 range cells, indicating a further drift of approximately 5.6 ns over the duration of the capture. This resulted from a drift in phase between the two GPSDOs 10 MHz outputs.

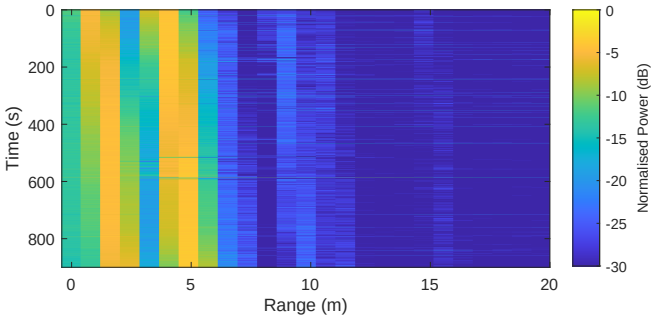

Fig. 6 Bistatic RTI plot for 15-minute radar experiment. The first two strong returns are the breakthrough from transmitter to receiver and the wall of the lab.

The phase series of the breakthrough for the bistatic capture is plotted in Fig.7, this provides a more detailed view of the phase dynamics between the radars. The bistatic phase series shows phase unwrapped results. We can observe a net phase drift of 112.4 radians over the 900 s experiment, equivalent to a drift of 7.4 ns. Fig.8 plots the Doppler spectrum of the breakthrough for both the monostatic and bistatic captures. As expected, the noise floor in the bistatic capture is higher than in the monostatic capture, approximately 7 dB worse in general. Moreover, the Doppler noise is around 10 dB worse in the region close to the carrier (< 50 Hz).

5 Conclusion

In this paper, the comparative performance between two different GPSDO technologies has been investigated. From the co-located lab measurements, the relative timing performance of the double OCXO Trimble devices was found to surpass the Rubidium Spectratime devices by nearly a factor of three. This could likely be attributed to GPS timing receivers internal to the Trimble devices using fixed, self-surveyed, GPS co-ordinates. However, the Spectratime devices periodically update their positions, introducing dynamic timing errors. Conversely, the short-to-medium term relative frequency stability between the Rubidium devices was measured to be 2-3 times better, see Fig.2. Furthermore, the relative phase noise performance of the Spectratime devices was measured to be at least 8 dB better than the Trimble devices. Consequently, if high accuracy Doppler velocity estimation, maximal coherent pulse integration or maximal SCV is required, the Spectratime devices would be the preferable choice for radar synchronisation. Nevertheless, the time accuracy between GPSDOs - which determines the radars range accuracy - will be the most limiting

factor in the use of these COTS GPSDOs. Assuming static time offsets, introduced by the GPS receiver internal delays and self-survey errors are removed, time drifts of the order of < ±4.2 ns and < ±11.4 ns should be expected for the Trimble and Spectratime devices respectively. If the requirement is to synchronise to within the radar range resolution, then the Trimble devices would theoretically be appropriate for radar bandwidths of < 70 MHz and the Spectratime devices for bandwidths of < 26 MHz. That said, the use of separate antennas, over large bistatic baselines with different ambient temperatures will likely considerably deteriorate the relative timing performance over that measured in the lab [1]. To that end, future outdoor ARESTOR radar experiments will be conducted with both GPSDO models integrated into the synchronisation system to investigate the synchronisation performance in non-ideal lab conditions.

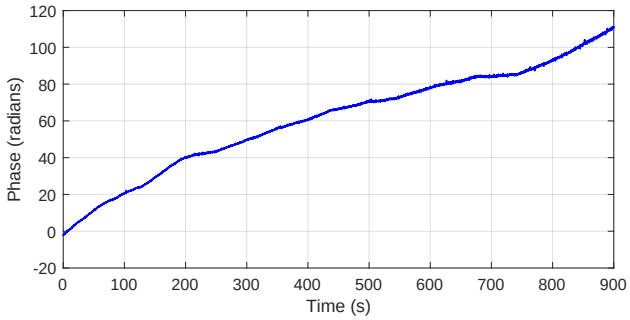

Fig. 7 Bistatic unwrapped phase series for 15-minute period. The phase drift of 112.4 radians at 2.42 GHz, equals a time drift of 7.4 ns. Comparable to an 8.22×10^{-12} frequency offset over the 900 s experiment.

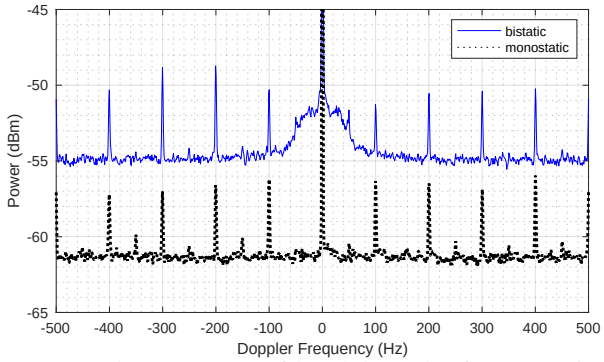

Fig. 8 Doppler Spectrum of breakthrough of monostatic and bistatic captures. The Doppler noise floor, referenced to the carrier, is 7 dB worse in the bistatic case. Spurious Doppler frequencies at multiples of 100 Hz are observed in the monostatic node and bistatic node captures.

6 Acknowledgements

The authors would like to acknowledge the UK Defence Science and Technology Laboratory (DSTL) for continuing to provide PhD sponsorship for the research into active and passive multistatic radar networks.

References

[1] Sandenbergh, J.S, “Synchronising Coherent Networked Radar using Low-Cost GPS-Disciplined Oscillators”. PhD thesis, University of Cape Town, 2019

[2] Sandenbergh, J.S, “Synchronising Coherent Networked Radar using Low-Cost GPS-Disciplined Oscillators”. PhD thesis, University of Cape Town, 2019

[3] Sandenbergh, J., Inggs, M., "Synchronizing network radar using all-in-view GPS-disciplined oscillators," 2017 IEEE Radar Conference (RadarConf), 2017, pp. 1640-1645.

[4] Inggs, M.R., Lewis, S., Palamà, R., et al., “Report on the 2018 Trials of the Multistatic NeXtRAD Dual Band Polarimetric Radar.” 2019 IEEE Radar Conference, RadarConf 2019. N.p., 2019.

[5] Weib M., Synchronisation of bistatic radar systems. 2004 IEEE International Geoscience and Remote Sensing Symposium, 2004, 1750–1753 vol.3.

[6] Willis N.J, ‘Bistatic Radar’, Raleigh, N.C: SciTech, 2005. Print.

[7] Lewis, S., Inggs, M.R., “Synchronization of Coherent Netted Radar Using White Rabbit Compared With One-Way Multichannel GPSDOs.” IEEE transactions on aerospace and electronic systems 57.3 2021: 1413–1422.

[8] Bovey, C. K, Horne, C. P., “Synchronization aspects for bistatic radars,” in Radar - 87; Proceedings of the International Conference, Jan. 1987, pp. 22–25.

[9] Auterman, J.L, ‘Phase stability requirements for a bistatic SAR system’, IEEE International Radar Conference, Atlanta, GA: IEEE,1984, pp. 48–52

[10] ‘Thunderbolt E GPS Disciplined Clock’, https://timing.trimble.com/wp-content/uploads/thunderbolt-e-gps-disciplined-clock-datasheet.pdf, accessed 28 March 2022.

[11] ‘Patented Smart LNRClok-1500’, https://www.orolia.com/wp-content/uploads/2021/07/isync_lnr_grclok_1500_manual_1-1.pdf, accessed 28 March 2022

[12] Weiss, M.A., Petit, G., Jiang, Z., “A Comparison of GPS Common-View Time Transfer to All-in-View.” Proceedings of the IEEE International Frequency Control Symposium and Exposition, vol. 2005, 2005, pp. 324–28.

[13] Lombardi, M.A, Novick, N.A., Zhang, V.S, “Characterizing the Performance of GPS Disciplined Oscillators with Respect to UTC(NIT).” Proceedings of the 2005 IEEE International Frequency Control Symposium and Exposition, 2005. IEEE, 2005. 677–684.

[14] ‘K+K FXE Phase + Frequency Meter’, http://kpluskmesstechnik.de/products/fxe_19.htm, accessed 29 March 2022

[15] Beasley, P.J, Ritchie, M.A., “bladeRAD: Development of an Active and Passive, Multistatic Enabled, Radar System” 2021 IEEE European Radar Conference (EuRAD), 2022, Print.

[16] Peters, N., Horne, C., Ritchie, M.A., “ARESTOR: A Multi-Role RF Sensor Based on the Xilinx RFSoC”, 2021 IEEE European Radar Conference (EuRAD), 2022, Print.